Acta Mech
https://doi.org/10.1007/s00707-025-04230-y

ORIGINAL PAPER

Hadj Youzera · Sid Ahmed Meftah · Abdelouahed Tounsi · Mohamed Abdelaziz Salem · Khaled Mohamed Khedher · Murat Yaylacı

Free vibration analysis of sandwich cylindrical shells with functionally graded carbon nanotube-reinforced composite face sheets using the differential quadrature (DQ) method

Received: 3 December 2024 / Revised: 22 December 2024 / Accepted: 27 December 2024
© The Author(s), under exclusive licence to Springer-Verlag GmbH Austria, part of Springer Nature 2025

Abstract This study investigates the free vibration behavior of cylindrical shell with a stiff core and functionally graded carbon nanotube-reinforced composite (FG-CNTRC) face sheets. Both uniformly distributed CNT reinforced (UD-CNT) and functionally graded CNT reinforced (FG-CNT) in the thickness direction are used to examine their impact on the vibration characteristics of sandwich cylindrical shells. The governing differential equations of motions are derived using Hamilton's principle. These equations are solved using the differential quadrature (DQ) method to calculate the natural frequencies of the sandwich cylindrical shell. This approach allows for the consideration of various support configurations of the sandwich cylindrical beams. A comprehensive parametric study is performed to explore the influence of carbon nanotube volume fraction, core-to-face sheet thickness ratio, slenderness ratio, and end supports on the free vibration behavior of cylindrical shells with functionally graded carbon nanotube-reinforced composite (FG-CNTRC) face sheets. The results show that the effects of carbon nanotubes and other geometric factors significantly influence the dimensionless frequencies of the sandwich cylindrical shells.

H. Youzera
Laboratoire d'Etude des Structures et de Mécanique des Matériaux, Département de Génie Civil, Faculté des Sciences et de la Technologie, Université Mustapha Stambouli, Mascara, Algeria

S. A. Meftah
Laboratoire des Structures et Matériaux Avancés dans le Génie Civil et Travaux Publics, Université Djillali Liabes, Sidi Bel Abbès, Algeria

A. Tounsi (✉)
Department of Civil and Environmental Engineering, King Fahd University of Petroleum & Minerals, Eastern Province, 31261 Dhahran, Saudi Arabia
e-mail: tou_abdel@yahoo.com

A. Tounsi
Material and Hydrology Laboratory, Civil Engineering Department, Faculty of Technology, University of Sidi Bel Abbes, Sidi Bel Abbès, Algeria

M. A. Salem
Department of Mechanical Engineering, College of Engineering, King Khalid University, 61421 Abha, Saudi Arabia

K. M. Khedher
Department of Civil Engineering, College of Engineering, King Khalid University, 61421 Abha, Saudi Arabia

M. Yaylacı
Department of Civil Engineering, Recep Tayyip Erdogan University, 53100 Rize, Turkey

M. Yaylacı
Faculty of Turgut Kıran Maritime, Recep Tayyip Erdogan University, 53900 Rize, Turkey

Published online: 15 January 2025

1 Introduction

Due to their excellent mechanical properties and diverse applications, composite structures, including functionally graded material (FGM) structures and functionally graded carbon nanotubes (FGCNT), have been extensively studied in various forms, such as beams, plates, and shells. Previous studies have mainly concentrated on isotropic and laminated composite structures. Soldatos and Hadjigeorgiou [1] studied the free vibration of a homogeneous isotropic thick cylindrical shell by using a new iterative approach to solve the governing equations of three-dimensional linear elasticity. Zukas and Vinson [2] investigated the behavior of multilayered circular, cylindrical shells subjected to arbitrary axisymmetric thermal and mechanical loads. Spillers [3] studied the buckling load and the flexural response of laminated thin cylindrical shell layers connected by springs under axisymmetric static loading. Bert et al. [4] investigated analytically the dynamic instability of simply supported, finite-length, orthotropic circular cylindrical shells subjected to uniformly distributed cyclic axial loading and including the effects of TSD. Based on the refined higher-order shear deformation theory (RHOST), Khalili et al. [5] presented an excellent study on free vibration analysis of simply supported–simply supported and clamped–clamped homogenous isotropic circular cylindrical using the Galerkin method for solving the equations of motion by using the first-order shear deformation theory, a unified vibration model of fiber-reinforced polymer (FRP) cylindrical shell with functionally graded porous graphene platelets (FGPGP) coating is proposed by Li et al.[6]. Free vibrations of a cylindrical shell constructed from a composite material reinforced with graphene platelets have been analyzed through an analytical approach by Baghbadorani and Kiani [7]. Qin et al. [8] performed a free vibration analysis on thick functionally graded porous graphene platelet-reinforced composite (FGP-GPLRC) cylindrical shells that are embedded in elastic foundations. Their approach combined the Rayleigh–Ritz method with an artificial spring technique to achieve the analysis. Azarafza et al. [9] examined the free vibration characteristics of composite cylindrical shells reinforced with carbon nanotubes and grid-stiffened under various boundary conditions. Based on an isogeometric method, Zhang et al. [10] conducted an analysis on the free vibration characteristics of sector cylindrical shells incorporating reinforcements of carbon nanotubes and functionally graded materials.Tang et al. [11] discussed the effect on the nonlinear boundary model on the forced vibration of thin-wall cylindrical shell, where the displacements in three directions represented by trigonometric functions. Orthotropic cylindrical shells under external pressures were studied by Sofiyev and Kuruoglu [12] to examine their behavior in vibration and buckling problems using the shear deformation shell theory (SDST). Alibeigloo and Jafarian [13] carried out the bending and free vibration of carbon nanotubes-reinforced composite (CNTRC) cylindrical shell using the three-dimensional theory. Based on the artificial spring technology, Miao et al.[14] analyzed the free vibrations of nanocomposite laminated cylindrical shells reinforced by carbon nanotubes (CNTs) under arbitrary boundary conditions using the first-order shear deformation theory (FSDT). Babaei and Jafari [15] investigated the vibrations of cylindrical-conical shells composed of functionally graded carbon nanotubes by applying Love shell assumptions and classical shell theory. Based on the methods of harmonic differential quadrature (HDQ), discrete singular convolution (DSC), Love's shell theory, and first-order shear deformation theory (FSDT), Baltacıoğlu and Civalek [16] examined the vibrations of cylindrical-conical shells made from functionally graded carbon nanotube-reinforced (CNTR) circular cylindrical panels. Chakraborty et al. [17] investigated the buckling, postbuckling, and vibration behavior of CNT-reinforced functionally graded laminated composite cylindrical shell panels using a semi-analytical approach. Hosseini and Kolahchi [18] created a mathematical model to study the seismic behavior of submerged cylindrical shells under hygrothermal loading. Alibeigloo and Zanoosi [19] analyzed the sandwich cylindrical shell with piezoelectric sensor and actuator layers subjected to under thermo-electro-mechanical load.Kiani et al. [20] investigated the impact of parameters like CNT distribution, volume fraction, and temperature variations on the natural frequencies and dynamic responses of composite sandwich cylindrical shells featuring porous cores and functionally graded carbon nanotubes. Pradhan et al. [21] investigated the free vibration of functionally graded material (FGM) cylindrical shells with different boundary conditions under temperature environment loads. Utilizing sinusoidal shear deformation theory (SSDT) and the Rayleigh–Ritz method, Wang et al. [22] conducted an elegant study on the free vibration analysis of functionally graded (FG) porous cylindrical shells under various boundary conditions. Chen and Ahmed [23] conducted a comprehensive analysis of the nonlinear vibration behavior of graphene nanoplatelet-reinforced composite plates supported on an elastic foundation, using the multiple scales method. Khoddami Maraghi and Arshid [24] studied the vibrational behavior of variable-thickness FG porous beams with graphene-reinforced nanocomposite facesheets, supported by an elastic foundation. Yan and Babaei [25] extensively studied the vibration and buckling behavior of a sandwich arch with titanium alloy face sheets and a metal foam core, using a new porosity-dependent model. Cho [26] investigated the

nonlinear vibration characteristics of functionally graded CNT-reinforced composite (FG-CNTRC) cylindrical shell panels on an elastic foundation, incorporating first-order shear deformation theory. Allahyari et al. [27] established the dynamic buckling behavior of truncated conical shells made of carbon nanotube composite beams using the differential quadrature method and Bolotin's method. Zhihua Cui et al. [28] presented a comprehensive study of the structural behavior of nanoparticle-reinforced nanocomposite porous beams under sinusoidal transverse dynamic forces Based on a new finite element formulation, Özdemir et al. [29] studied the free vibration behavior of rotating composite beams reinforced with carbon nanotubes (CNTs) under uniform thermal loading. Zhang et al. [30] used a generalized differential quadrature (GDQ) method to present the vibration analysis of trapezoidal sandwich plates with a 3D-graphene foam reinforced polymer matrix composite (GrF-PMC) core and FG wavy CNT-reinforced face sheets. Based on the Kelvin-Voigt model, Long et al. [31] investigated the static and dynamic bending of balls reinforced with CNTs, considering the agglomeration effect. Nonlinear vibration analysis of functionally graded nanocomposite spherical shells reinforced with graphene platelets is presented by Wu [32]. The natural frequency behavior of graphene platelets reinforced composite (GPL-RC) joined truncated conical-cylindrical-conical shells resting on a Winkler-type elastic foundation is presented by Wang et al. [33], using a finite element procedure and the Rayleigh–Ritz formulation. Alambeigi et al. [34] investigated the free vibration behavior of a micro-sandwich beam composed of five layers: a functionally graded (FG) porous core, a nanocomposite reinforced with carbon nanotubes (CNTs), and piezomagnetic/piezoelectric layers, subjected to magnetoelectrical potential and resting on a silica aerogel foundation. Based on Reddy's plate model, Ding et al. [35] investigated wave propagation in functionally graded carbon nano-reinforced composite (FG-CNTRC) plates under the influence of temperature. Using HSDT and the Ritz method, Emdadi et al. [36] investigated the impact of surface stress on the buckling behavior of a porous microcomposite annular sandwich plate, with two face layers made of carbon nanotubes (CNTs) and a functionally graded porous core.

In this study, the differential quadrature (DQ) method is utilized to determine the natural frequency of a cylindrical sandwich shell with a stiff core and functionally graded carbon nanotube-reinforced composite (FG-CNTRC) face sheets under various boundary conditions. This study examines how changes in nanotube volume fraction, core-to-face sheet thickness ratio, slenderness ratio, and end supports impact the vibration behaviors of sandwich cylindrical shells with FG-CNTRC face sheets. Numerical results are provided, comparing these effects and discussing various geometric and boundary conditions along with CNT distributions.

The objective is to examine the impact of volume fractions, as well as the effects of carbon nanotube distribution and geometric parameters on the vibration behavior of sandwich cylindrical shells. The structure formed of FG-CNT present an excellent choice for high performance of engineering applications.

2 Sandwich beam with CNTRC face sheets

The geometry of the sandwich circular cylindrical shell with layers with carbon nanotube-reinforced face sheets are shown in Fig. 1. Indices R, L and h refer to the radius, length L, thickness of the sandwich structure, respectively. This sandwich comprises two CNTRC face sheets of equal thickness h_f separated by a stiff core layer of thickness hc. According to the rule of mixtures, the material properties are determined

$$E_{11} = \eta_1 V_{cn} E_{11}^{cn} + V_m E_m \tag{1}$$

$$\frac{\eta_2}{E_{22}} = \frac{V_{cn}^*}{E_{22}^{cn}} + \frac{V_m}{E_{22}^m} \tag{2}$$

$$\frac{\eta_3}{G_{12}} = \frac{V_{cn}^*}{G_{12}^{cn}} + \frac{V_m}{G_m} \tag{3}$$

$$\upsilon_{12} = V_{cn}\upsilon_{cn} + V_m\upsilon_m \tag{4}$$

$$\rho = V_{cn}\rho_{cn} + V_m\rho_m \tag{5}$$

where E_{11}^{cn}, E_{22}^{cn}, G_{12}^{cn}, υ_{cn} and ρ_{cn} are the elastic moduli, shear moduli, Poisson's ratio and density of the CNT, respectively. E_m, G_m, υ_m and ρ_m are the material properties of the matrix.

The properties of the FG-CNTRC face sheet vary linearly across the thickness according to the given distribution.

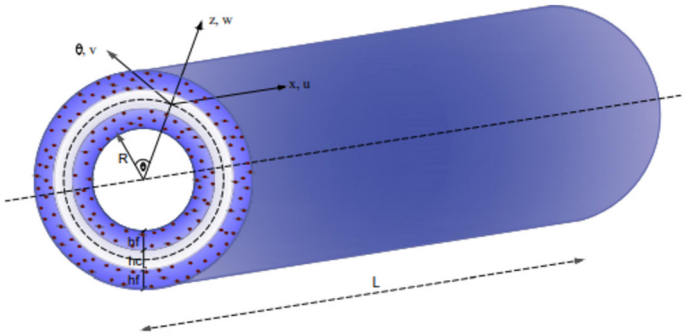


Fig. 1 Configuration of sandwich cylindrical shell with CNTRC face sheets

For the top layer

$$V_{cn} = \frac{-(2z + h_c)}{h_f} V_{cn}^* \tag{6}$$

For the bottom layer

$$V_{cn} = \frac{(2z - h_c)}{h_f} V_{cn}^* \tag{7}$$

And

$$V_{cn}^* = \frac{w_{cn}}{w_{cn} + (\rho_{cn}/\rho_m) - (\rho_{cn}/\rho_m) w_{cn}} \tag{8}$$

In which w_{cn} represents the mass fraction of CNT.

2.1 Theory and formulation

The material properties include Young's modulus E, Poisson's ratio ν, and mass density ρ. The orthogonal coordinate system (x,θ,z) is established at the midplane of the cylindrical shell. It is assumed that the principal material direction is aligned with the coordinate axes. The displacements of an arbitrary point in the cylindrical shell along the x, θ and z-axes, denoted by U(x, θ, z,t),V(x, θ, z,t) and W(x, θ, z,t) that represent the axial, circumferential and radial displacement respectively.

Based on From Love's first approximation theory [22], the strain–displacement relations can be defined as:

$$\begin{Bmatrix} \varepsilon_x \\ \varepsilon_\theta \\ \varepsilon_{x\theta} \end{Bmatrix} = \begin{Bmatrix} \frac{\partial u}{\partial x} \\ \frac{1}{R}\left(\frac{\partial v}{\partial \theta} + w\right) \\ \frac{\partial v}{\partial x} + \frac{1}{R}\frac{\partial u}{\partial \theta} \end{Bmatrix} \tag{9}$$

$$\begin{Bmatrix} k_x \\ k_\theta \\ \gamma_{x\theta} \end{Bmatrix} = -\begin{Bmatrix} \frac{\partial^2 w}{\partial x^2} \\ \frac{1}{R^2}\left(\frac{\partial^2 w}{\partial \theta^2} - \frac{\partial v}{\partial \theta}\right) \\ \frac{1}{R}\left(\frac{\partial^2 w}{\partial x \partial \theta} - \frac{\partial v}{\partial x}\right) \end{Bmatrix} \tag{10}$$

The linear-stress–strain relationship can be expressed as follows:

$$\begin{Bmatrix} \sigma_x \\ \sigma_\theta \\ \sigma_{x\theta} \end{Bmatrix} = \begin{bmatrix} Q_{11} & Q_{12} & 0 \\ Q_{12} & Q_{22} & 0 \\ 0 & 0 & Q_{66} \end{bmatrix} \left(\begin{Bmatrix} \varepsilon_x \\ \varepsilon_\theta \\ \varepsilon_{x\theta} \end{Bmatrix} + z \begin{Bmatrix} k_x \\ k_\theta \\ 2\gamma_{x\theta} \end{Bmatrix} \right) \tag{11}$$

The force and moment resultants can be written as:

$$\begin{Bmatrix} N_x \\ N_\theta \\ N_{x\theta} \end{Bmatrix} = \begin{bmatrix} A_{11} & A_{12} & 0 \\ A_{12} & A_{22} & 0 \\ 0 & 0 & A_{66} \end{bmatrix} \begin{Bmatrix} \frac{\partial u}{\partial x} \\ \frac{1}{R}\left(\frac{\partial v}{\partial \theta} + w\right) \\ \frac{\partial v}{\partial x} + \frac{1}{R}\frac{\partial u}{\partial \theta} \end{Bmatrix} + \begin{bmatrix} B_{11} & B_{12} & 0 \\ B_{12} & B_{22} & 0 \\ 0 & 0 & B_{66} \end{bmatrix} \begin{Bmatrix} -\frac{\partial^2 w}{\partial x^2} \\ -\frac{1}{R^2}\left(\frac{\partial^2 w}{\partial \theta^2} - \frac{\partial v}{\partial \theta}\right) \\ -\frac{2}{R}\left(\frac{\partial^2 w}{\partial x \partial \theta} - \frac{\partial v}{\partial x}\right) \end{Bmatrix} \tag{12}$$

$$\begin{Bmatrix} M_x \\ M_\theta \\ M_{x\theta} \end{Bmatrix} = \begin{bmatrix} B_{11} & B_{12} & 0 \\ B_{12} & B_{22} & 0 \\ 0 & 0 & B_{66} \end{bmatrix} \begin{Bmatrix} \frac{\partial u}{\partial x} \\ \frac{1}{R}\left(\frac{\partial v}{\partial \theta} + w\right) \\ \frac{\partial v}{\partial x} + \frac{1}{R}\frac{\partial u}{\partial \theta} \end{Bmatrix} + \begin{bmatrix} D_{11} & D_{12} & 0 \\ D_{12} & D_{22} & 0 \\ 0 & 0 & D_{66} \end{bmatrix} \begin{Bmatrix} -\frac{\partial^2 w}{\partial x^2} \\ -\frac{1}{R^2}\left(\frac{\partial^2 w}{\partial \theta^2} - \frac{\partial v}{\partial \theta}\right) \\ -\frac{2}{R}\left(\frac{\partial^2 w}{\partial x \partial \theta} - \frac{\partial v}{\partial x}\right) \end{Bmatrix} \tag{13}$$

Aij, B_{ij} and D_{ij} are the extensional, coupling and bending stiffnesses:

$$A_{ij} = A_{ij}^{(1)} + A_{ij}^{(2)} + A_{ij}^{(3)} = \int_{-h_t/2}^{-h_c/2} Q_{ij}dz + \int_{h_c/2}^{h_c/2} Q_{ij}dz + \int_{h_c/2}^{h_t/2} Q_{ij}dz \tag{14}$$

$$B_{ij} = B_{ij}^{(1)} + B_{ij}^{(2)} + B_{ij}^{(3)} = \int_{-h_t/2}^{-h_c/2} Q_{ij}z dz + \int_{h_c/2}^{h_c/2} Q_{ij}z dz + \int_{h_c/2}^{h_t/2} Q_{ij}z dz \tag{15}$$

$$D_{ij} = D_{ij}^{(1)} + D_{ij}^{(2)} + D_{ij}^{(3)} = \int_{-h_t/2}^{-h_c/2} Q_{ij}z^2 dz + \int_{h_c/2}^{h_c/2} Q_{ij}z^2 dz + \int_{h_c/2}^{h_t/2} Q_{ij}z^2 dz \tag{16}$$

The principle of Hamilton's is used to derive the equations of motion. The Hamilton's principle in the present sandwich structure circumstances reads:

$$\delta \int_{t_0}^{t_1} (U_s - K_t) = 0 \tag{17}$$

By inserting the strain expression and calculating the integrals through the thickness in Eq. (11), the strain energy for the sandwich beam rewritten as:

$$U_s = \int_v \sigma_{ij}\varepsilon_{ij} dv = \frac{1}{2}\int_v \left(\{\varepsilon\}^T[A]\{\varepsilon\} + \{\varepsilon\}^T[A]\{k\} + \{k\}^T[A]\{\varepsilon\} + \{k\}^T[A]\{k\}\right) R\, dz\, d\theta\, dx \tag{18}$$

The kinetic energy related to the considered sandwich beam structure is:

$$K_t = \frac{1}{2}\int_v \rho\left(\left(\frac{\partial u}{\partial t}\right)^2 + \left(\frac{\partial v}{\partial t}\right)^2 + \left(\frac{\partial w}{\partial t}\right)^2\right) R\, dz\, d\theta\, dx \tag{19}$$

The equilibrium equations of motion for a thin cylindrical shell can be written as:

$$\frac{\partial N_x}{\partial x} + \frac{1}{R}\frac{\partial N_{x\theta}}{\partial \theta} = \rho_t \frac{\partial^2 u}{\partial t^2} \tag{20}$$

$$\frac{\partial N_{x\theta}}{\partial x} + \frac{1}{R}\frac{\partial N_\theta}{\partial \theta} + \frac{1}{R}\frac{\partial M_{x\theta}}{\partial x} + \frac{1}{R^2}\frac{\partial M_\theta}{\partial \theta} = \rho_t \frac{\partial^2 v}{\partial t^2} \tag{21}$$

$$\frac{\partial^2 M_x}{\partial x^2} + \frac{2}{R}\frac{\partial^2 M_{x\theta}}{\partial x \partial \theta} + \frac{1}{R^2}\frac{\partial^2 M_\theta}{\partial \theta^2} - \frac{N_\theta}{R} = \rho_t \frac{\partial^2 w}{\partial t^2} \tag{22}$$

A general relation for the displacement fields of a thin cylindrical shell with general boundary conditions can be written as:

$$u(x,\theta,t) = \xi_1(x)\cos(r\theta)e^{i\omega t} \tag{23.1}$$

$$v(x,\theta,t) = \xi_2(x)\sin(r\theta)e^{i\omega t} \tag{23.2}$$

Table 1 Material properties for SWCNT and matrix

Matrix	CNTRC facings
$E_{11}^{cn} = 5{,}6466$ Tpa	$E_m = 113{,}8$ Gpa
$E_{22}^{cn} = 7{,}08$ Tpa	$\rho_{cn} = 4430$ kg/m^3
$G_{12}^{cn} = 1{,}9448$ Tpa	$\upsilon_m = 0{,}342$
$\rho_{cn} = 1400$ kg/m^3	/
$\upsilon_{cn} = 0{,}175$	/

Table 2 CNT efficiency parameters

V_{cnt}	0,12	0,17	0,28
η_1	0,142	0,142	0,141
η_2	0,137	1,626	1,585
η_3	0,715	1,138	1,109

$$w(x,\theta,t) = \xi_3(x)\cos(r\theta)e^{i\omega t} \tag{23.3}$$

Substituting Eqs. (23) into Eqs. (20–22), the governing equations can be rewritten as:

$$\alpha_{111}\xi_1 + \alpha_{112}\xi_1^{(2)} + \alpha_{121}\xi_2^{(1)} + \alpha_{131}\xi_3^{(1)} + \alpha_{132}\xi_3^{(3)} = -\rho^t\omega^2\xi_1 \tag{24}$$

$$\alpha_{211}\xi_1^{(1)} + \alpha_{221}\xi_2 + \alpha_{222}\xi_2^{(2)} + \alpha_{231}\xi_3 + \alpha_{232}\xi_3^{(2)} = -\rho_t\omega^2\xi_2 \tag{25}$$

$$\alpha_{311}\xi_1^{(1)} + \alpha_{132}\xi_1^{(3)} + \alpha_{321}\xi_2 + \alpha_{322}\xi_2^{(2)} + \alpha_{331}\xi_3 + \alpha_{332}\xi_3^{(2)} + \alpha_{333}\xi_3^{(4)} = -\rho_t\omega^2\xi_3 \tag{26}$$

where $\xi^{(i)}$ denote the ith order derivative ξ, and α $(ijk)$are the constant coefficients defined in the Appendix.

2.2 Solution procedure

The GDQ is a very effective numerical technique for solving différential equations by the grid point displacements. With the aid of GDQ, one can have a discrete dynamical system, moreover the admissible displacement functions are unnecessary. Thus, the GDQ is used to research the natural vibration of the cylindical shell with the general boundary conditions.

The displacement components $\xi^{(i)}$ and their kth derivatives with respect to can be approximated by:

$$\{\xi_1,\xi_2,\xi_3\} = \sum_{m=1}^{N} l_m(\varsigma)\{\xi_{1,m},\xi_{2,m},\xi_{3,m}\}, \tag{27}$$

$$\frac{\partial^k}{\partial\varsigma^k}\{\xi_1,\xi_2,\xi_3\}|_{\varsigma=\varsigma_i} = \sum_{m=1}^{N} C_{im}^{(k)}\{\xi_{1,m},\xi_{2,m},\xi_{3,m}\} \tag{28}$$

l_m is the Lagrange interpolation polynomials. The weighting coefficients $C_{im}^{(k)}$ can be calculated using recursive formula [37, 38]. N is the total number of nodes distributed along the axis according to a cosine pattern given below.

$$\varsigma_i = \frac{1}{2}\left\{1 - \cos\left[\frac{\pi(i-1)}{N-1}\right]\right\}L, \quad i = 1,2,...,N \tag{29}$$

To implement the GDQ method, and after performing spatial discretization, the governing equations (Eqs. 24–26) can be rewritten as:

$$\alpha_{111}\xi_{1,m} + \alpha_{112}\sum_{j=1}^{N} C_{ij}^{(2)}\xi_{1,m} + \alpha_{121}\sum_{j=1}^{N} C_{ij}^{(1)}\xi_{2,m} + \alpha_{131}\sum_{j=1}^{N} C_{ij}^{(1)}\xi_{3,m} + \alpha_{132}\sum_{j=1}^{N} C_{ij}^{(3)}\xi_{3,m} + \rho^t\omega^2\xi_{1,m} = 0 \tag{30}$$

Table 3 Comparison of non-dimensional natural frequencies ($\widetilde{\omega} = R\omega\sqrt{(1-\upsilon^2)\rho/E}$) for isotropic cylindrical shell

r	SS				CC				CS			
	(m = 1 Soldatos [1]	L/R = 20 Pradhan [21]	h/R = 0.01) Wang [22]	Present	(m = 1 Soldatos [1]	L/R = 20 Pradhan [21]	h/R = 0.002) Wang [22]	Present	(m = 1 Soldatos [1]	L/R = 20 Pradhan [21]	h/R = 0.002) Wang [22]	Present
1	0,0161	0,0168	0,0161	0.01610	0,0344	0,0342	0,034	0.032827	0,02483	0,023974	0,0248	0.02391
2	0,0093	0,0097	0,0094	0.00936	0,012	0,0119	0,0119	0.011623	0,00841	0,008223	0,0084	0.00821
3	0,0221	0,023	0,0221	0.02208	0,0072	0,0072	0,0072	0.00707	0,005897	0,005842	0,0059	0.00584
4	0,0421	0,0439	0,0421	0.04207	0,009	0,0089	0,009	0.00900	0,008717	0,008705	0,0087	0.00870
5	0,0681	0,0709	0,068	0.06798	0,0137	0,0136	0,0137	0.01375	0,013682	0,013679	0,0137	0.01367

Table 4 Variations of minimum natural frequencies (Hz) with L/R for a UD-CNT cylindrical shell ($m = 1$, h/R = 0.05, Type 1–1-1)

L/R	CC			CS			SS		
	0,12	0,17	0,28	0,12	0,17	0,28	0,12	0,17	0,28
0,5	1780,074	1951,436	2273,711	1408,297	1541,294	1793,335	616,302	671,261	779,042
1	969,287	1054,522	1218,147	926,009	1007,241	1164,026	616,299	671,235	779,043
2	620,185	674,756	780,933	605,695	658,523	761,016	602,094	654,503	756,189
5	252,127	274,386	317,834	222,016	241,483	279,376	195,71	212,705	245,659
10	104,62	113,779	131,594	83.369	90.628	104,714	62.141	67.514	77.913
20	34.528	37.521	43.320	25.159	27.336	31.550	16.940	18.401	21.227
50	6.208	6.743	7.777	4.324	4.696	5.417	2.787	3.027	3.491
100	1.581	1.717	1.980	1.094	1.188	1.370	0.699	0.758	0.877

Table 5 Variations of minimum natural frequencies (Hz) with L/R for a FGV-CNT cylindrical shell ($m = 1$, h/R = 0.05, Type 1–1–1)

L/R	CC			CS			SS		
	0,12	0,17	0,28	0,12	0,17	0,28	0,12	0,17	0,28
0,5	1849,353	2045,18	2407,629	1450,61	1598,787	1612,847	616,796	672,29	781,669
1	977,013	1065,116	1233,632	930,249	1013,146	1236,515	616,806	672,276	781,675
2	621,266	676,408	783,953	606,23	659,437	762,751	602,383	655,007	757,313
5	252,391	274,837	318,8	222,172	241,756	279,991	195,761	212,806	245,921
10	104,691	113,902	131,865	83.407	90.695	104,866	62.150	67.534	77.965
20	34.539	37.540	43.365	25.166	27.348	31.577	16.942	18.404	21.237
50	6.209	6.744	7.780	4.324	4.697	5.419	2.787	3.027	3.491
100	1.581	1.717	1.981	1.094	1.188	1.370	0.7004	0.7604	0.876

Table 6 Variations of minimum natural frequencies (Hz) with various type of sandwich structures for a FGU-CNT cylindrical shell ($m = 1$, h/R = 0.05 and L/h = 20) For UD-CNT

h/R	CC			CS			SS		
	0,12	0,17	0,28	0,12	0,17	0,28	0,12	0,17	0,28
1*0*1	37.716	42.056	50.597	27.481	30.638	36.846	18.502	20.622	24.789
2*1*2	35.815	39.351	46.235	26.096	28.669	33.672	17.570	19.297	22.651
1*1*1	34.528	37.521	43.320	25.159	27.336	31.550	16.940	18.401	21.227
1*2*1	32.891	35.190	39.633	23.968	25.640	28.868	16.137	17.261	19.424
1*4*1	31.217	32.796	35.855	22.749	23.897	26.119	15.319	16.089	17.578
4*1*4	36.664	40.559	48.173	26.715	29.548	35.082	17.985	19.888	23.600

Table 7 Variations of minimum natural frequencies (Hz) with various type of sandwich structures for a FGU-CNT cylindrical shell ($m = 1$, h/R = 0.05and L/h = 20) For FGV-CNT

Type	CC			CS			SS		
	0,12	0,17	0,28	0,12	0,17	0,28	0,12	0,17	0,28
1–0–1	37.732	42.084	50.658	27.490	30.654	36.880	18.504	20.627	24.796
2–1–2	35.828	39.374	46.287	26.104	28.682	33.702	17.572	19.301	22.661
1–1–1	34.539	37.540	43.365	25.166	27.348	31.577	16.942	18.404	21.237
1–2–1	32.899	35.205	39.669	23.973	25.649	28.890	16.140	17.263	19.433
1–4–1	31.222	32.806	35.881	22.752	23.903	26.135	15.320	16.092	17.585
4–1–4	36.678	40.583	48.229	26.723	29.562	35.114	17.987	19.893	23.612

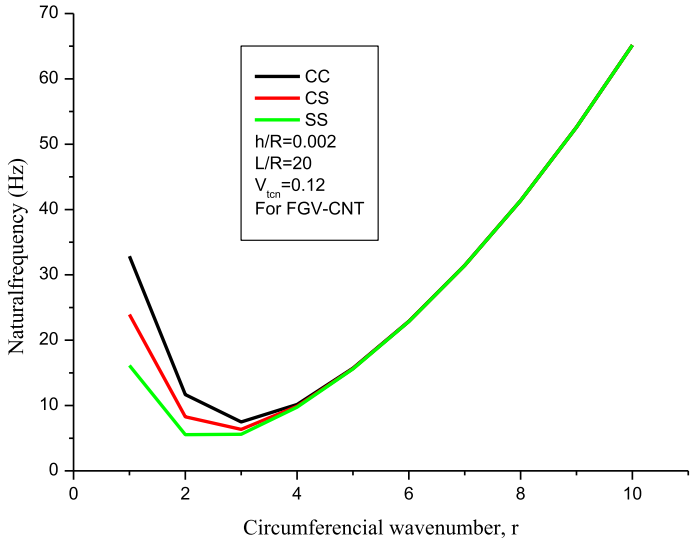


Fig. 2 Natural frequencies associated of 1-2-1 with various boundary conditions

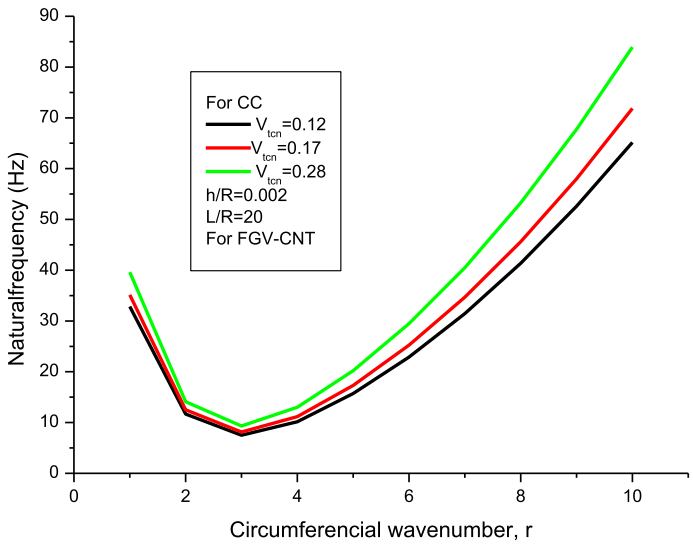


Fig. 3 Natural frequencies associated with various CNT efficiency parameters for 1-2-1 and CC type boundary condition

$$\alpha_{211}\sum_{j=1}^{N}C_{ij}^{(1)}\xi_{1,m}+\alpha_{221}\xi_{2,m}+\alpha_{222}\sum_{j=1}^{N}C_{ij}^{(2)}\xi_{2,m}+\alpha_{231}\xi_{3,m}+\alpha_{232}\sum_{j=1}^{N}C_{ij}^{(2)}\xi_{3,m}+\rho_t\omega^2\xi_2=0 \tag{31}$$

$$\alpha_{311}\sum_{j=1}^{N}C_{ij}^{(1)}\xi_{1,m}+\alpha_{132}\sum_{j=1}^{N}C_{ij}^{(3)}\xi_{1,m}+\alpha_{321}\xi_{2,m}+\alpha_{322}\sum_{j=1}^{N}C_{ij}^{(2)}\xi_{2,m}+\alpha_{331}\xi_{3,m}+\alpha_{332}\sum_{j=1}^{N}C_{ij}^{(2)}\xi_{3,m}$$
$$+\alpha_{333}\sum_{j=1}^{N}C_{ij}^{(4)}\xi_{3,m}+\rho_t\omega^2\xi_{3,m}=0 \tag{32}$$

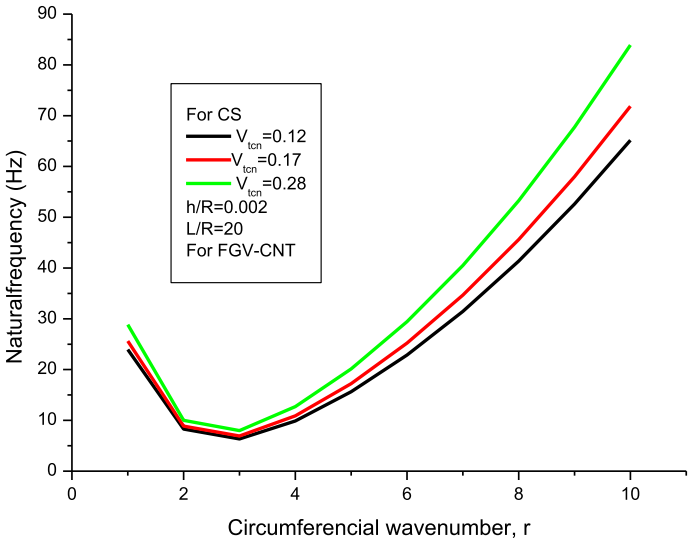


Fig. 4 Natural frequencies associated with various CNT efficiency parameters for 1-2-1 and CS type boundary condition

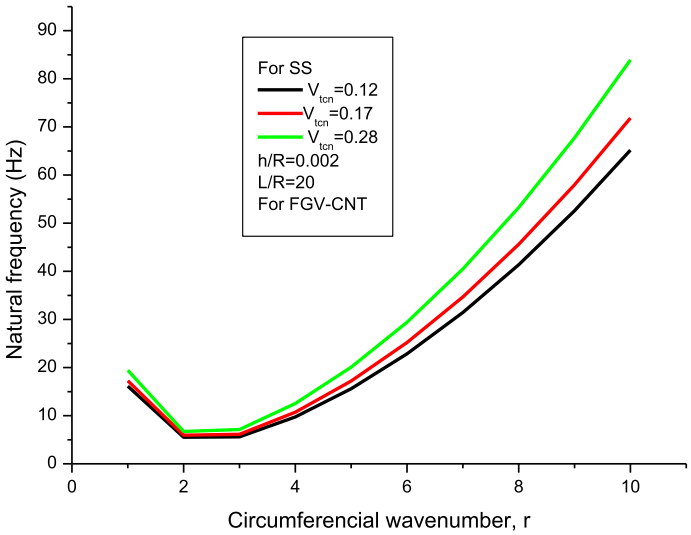


Fig. 5 Natural frequencies associated with various CNT efficiency parameters for 1-2-1 and SS type boundary condition

3 Results and discussion

In this study, the free vibration of sandwich cylindrical shells with functionally graded carbon nanotube-reinforced composite face sheets (Fig. 1) under various boundary conditions is examined. The main material and geometrical properties of the considered structure are presented in Tables 1 and 2.

To validate the analysis, the comparison results are listed in Tables 3, 4 and 5. As shown in Tables 3 and 4, the natural frequencies from this work agree with those in the literature. In the second part, the free vibration analysis of cylindrical shells with CNTRC facings is presented and discussed. Altogether, three boundary conditions have been considered in the study: clamped–clamped (CC), simply supported–simply supported (SS), clamped–simply supported (CS).

Table 3 presents the variations of minimum natural frequencies (Hz) for different h/R ratios for a UD-CNT cylindrical shell type, where the slenderness ratio is kept at h/R = 0.05 and the core-to-face sheet thickness ratio hc/hf = 1 that is to say 1–1–1.

It is observed that the natural frequencies of the sandwich cylindrical shell increases with an increase in the CNT volume fraction V_{cn} but decreases as the slenderness ratio L/R increases. The CC cylindrical shell has a higher natural frequency than the same CS and the last SS cylindrical shells. In Table 4, the cylindrical shell

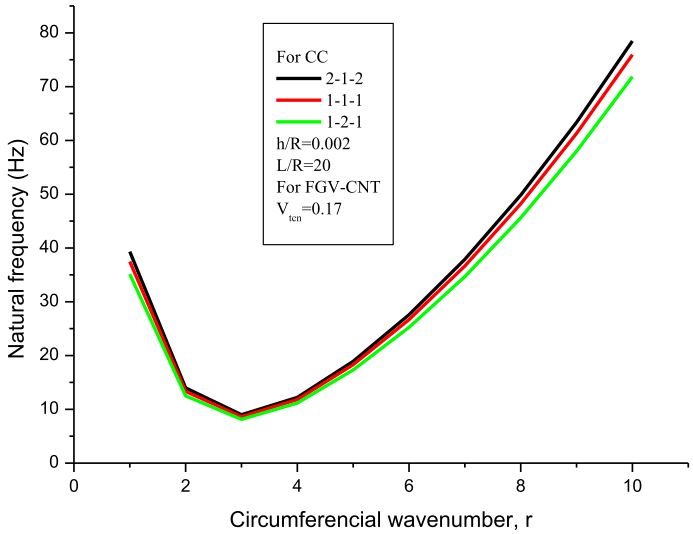


Fig. 6 Effect of core thickness on natural frequencies of CC sandwich structures

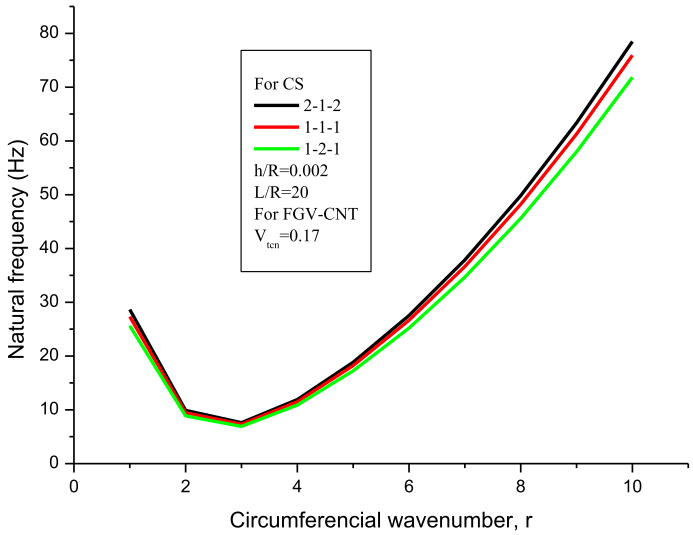


Fig. 7 Effect of core thickness on natural frequencies of CS sandwich structures

FGV-CNT has a higher natural frequency than the UD-CNT cylindrical shell type and also decreases as the slenderness ratio L/R increases. Natural frequencies of the sandwich cylindrical shell (h/R = 0.05,1–1–1 UD-CNT and FGV-CNT) subject to various boundary conditions are computed in Tables 4 and 5. The frequency first increases as the volume fraction increase and then increases as the L/R ratios increase for all boundary conditions and it is larger for the second case FGV-CNT. The effects of the different thickness on the frequencies for various boundary conditions are studied in Tables 6 and 7, is seen that the type of UD carbon nanotubes distribution for cylindrical shells has the lowest frequency while the other parameters are taken same value. As we can observe, the minimum natural frequencies (Hz) increase when the thickness of the middle layer decreases and the thickness of the top and bottom layers increases, and vice versa. Tables 8 and 9 show the variations in the fundamental natural frequencies with h/R ratios of FGM cylindrical shell. It is noted that the natural frequencies of the sandwich cylindrical shell increase as the CNT volume fraction increase and a small increase as the thickness ratio (h/R) becomes larger. The CC cylindrical shell demonstrates a higher natural frequency than both the CS and SS cylindrical shells.

Figures 2, 3, 4, 5, 6, 7 and 8 give the first natural frequency of FGV-CNT cylindical shell with various s boundary conditions. The results indicate that, with h/R = 0.002, L/R = 20, the frequencies for all boundary conditions initially decrease and then increase as the circumferential wavenumber n increases. This leads to

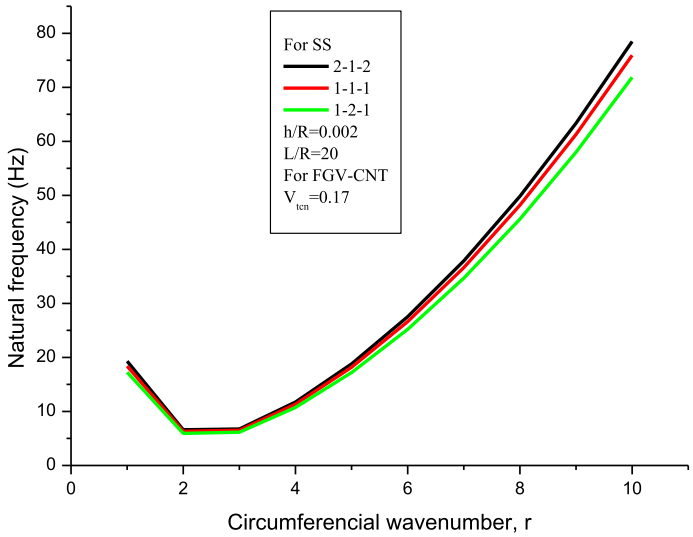


Fig. 8 Effect of core thickness on natural frequencies of SS sandwich structures

Table 8 Variations of minimum natural frequencies (Hz) with h/R for a UD-CNT cylindrical shell ($m = 1$, L/R = 20, Type 1-1-1)

h/R	CC			CS			SS		
	0,12	0,17	0,28	0,12	0,17	0,28	0,12	0,17	0,28
0,001	34.483	37.472	43.266	25.132	27.307	31.518	16.938	18.399	21.224
0,005	34.483	37.473	43.267	25.132	27.307	31.518	16.938	18.399	21.224
0,007	34.484	37.473	43.267	25.132	27.307	31.519	16.938	18.399	21.224
0,01	34.485	37.475	43.268	25.133	27.308	31.520	16.938	18.399	21.224
0,02	34.491	37.481	43.276	25.137	27.312	31.524	16.938	18.400	21.225
0,03	34.501	37.492	43.288	25.143	27.319	31.531	16.938	18.400	21.226
0,04	34.513	37.505	43.303	25.151	27.327	31.540	16.939	18.401	21.226
0,05	34.528	37.521	43.320	25.159	27.336	31.550	16.940	18.401	21.227

Table 9 Variations of minimum natural frequencies (Hz) with h/R for a FGV-CNT cylindrical shell ($m = 1$, L/R = 20, Type 1-1-1)

h/R	CC			CS			SS		
	0,12	0,17	0,28	0,12	0,17	0,28	0,12	0,17	0,28
0,001	34.490	37.487	43.305	25.136	27.315	31.541	16.940	18.402	21.234
0,005	34.490	37.487	43.306	25.136	27.316	31.542	16.940	18.402	21.234
0,007	34.491	37.488	43.306	25.137	27.316	31.542	16.940	18.402	21.234
0,01	34.492	37.489	43.308	25.137	27.317	31.543	16.940	18.402	21.234
0,02	34.499	37.497	43.316	25.142	27.321	31.548	16.940	18.402	21.234
0,03	34.509	37.508	43.329	25.148	27.328	31.556	16.940	18.403	21.235
0,04	34.523	37.523	43.346	25.156	27.337	31.566	16.941	18.404	21.236
0,05	34.539	37.540	43.365	25.166	27.348	31.577	16.942	18.404	21.237

the U-shaped frequency curves seen in Figs. 2, 3, 4, 5, 6, 7 and 8. The results in Fig. 2 indicate that, regardless of the boundary conditions, all frequencies converge as n becomes large.

Natural frequencies with CNT volume fraction varying from 0.12, 0.17 to 0.28 and hc = 2hf (1–2-1) for CC,CS and SS boundary conditions are presented in Fig. 3, 4 and 5. The fundamental frequencies of three boundary conditions are nearly for circumferential wavenumber n ≤ 3. However, as the circumferential wavenumber n increases, the effect of volume fraction V_{cn} appears larger especially $n \geq 3$, the difference also increases and becomes greater than 0.28, 0.17, and 0.12, respectively. The differences for the first mode frequencies of CC, CS and SS cylindrical shell depending on circumferential wavenumber are clearly appear, respectively.

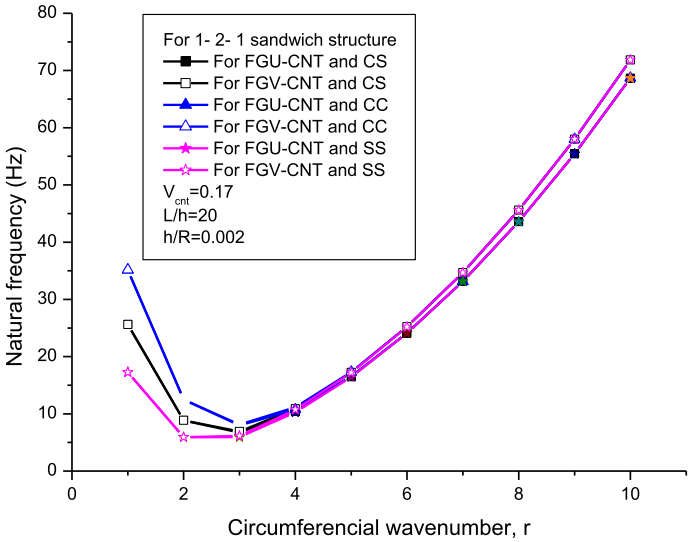


Fig. 9 Natural frequencies associated with various distributed carbon nanotube-reinforced face sheets with 1-2-1 sandwich structure

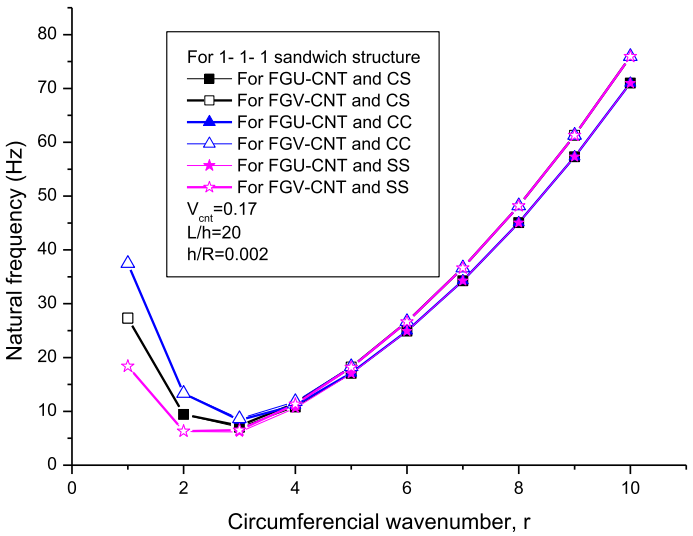


Fig. 10 Natural frequencies associated with various distributed carbon nanotube-reinforced face sheets with 1-1-1 sandwich structure

Figures 6, 7 and 8 show the effect of core thickness on natural frequencies of cylindrical shell with various boundary conditions. The effect of the hc/hf on the difference of fundamental natural frequency becomes more significant for the case of r > 6. Whenever the thickness of the middle layer is less than that of the outer layers, the frequency increases. This reflects the dominance of stiffness in the reinforced by carbon nanotube-reinforced by outer layers over the less stiff middle layer.

Natural frequencies associated with various hc/h ratios (1–2-1,1–1–1 and 2–1–2) sandwich structure and with CC, CS and SS boundary conditions for deferent circumferential wavenumber are presented in Figs. 9, 10 and 11. The fundamental frequency of the sandwich cylindrical shell with FG-CNTRC face sheets is slightly higher than that of the beam with UD-CNTRC face sheets. Also, the C–C sandwich beam has a higher natural frequency than its CS and SS. And this difference is clearly evident in the structure's increased stiffness, meaning for 2–1-2.

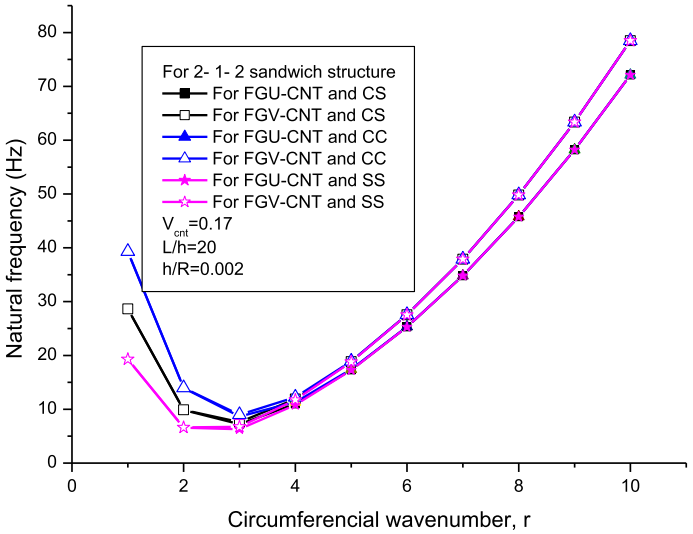


Fig. 11 Natural frequencies associated with various distributed carbon nanotube-reinforced face sheets with 2-1-2 sandwich structure

4 Conclusion

The natural vibration of sandwich cylindrical shell beams with CNTRC face sheets has been studied using the DQ (Differential Quadrature) method. Thorough parametric study was undertaken to examine how the CNT volume fraction, core-to-face sheet thickness ratio, slenderness ratio, and end support conditions affect the free vibration characteristics of stiffened-core sandwich cylindrical shell with CNTRC face sheets. Numerical findings demonstrate that the natural frequencies are notably influenced by the CNT volume fraction, slenderness ratio, and end support conditions, whereas the impact of the L/R ratio is comparatively less significant. The numerical results also indicate that the sandwich structure with FG-CNTRC face sheets exhibits superior vibration performance compared to the cylindrical shell with UD-CNTRC face sheets.

Funding The Authors extend their appreciation to the Deanship Scientific Research at King Khalid University for funding this work through large group Research Project under grant number: RGP2/494/45.

Data availability No Data associated in the manuscript.

Declarations

Conflict of interest The authors declare no conflict of interest in preparing this article.

Appendix

$$\alpha_{111} = -A_{66}\frac{r^6}{R^2}$$

$$\alpha_{112} = A_{11}$$

$$\alpha_{121} = (B_{12} + 2B_{66})\frac{r}{R^2} + (A_{66} + A_{12})\frac{r}{R}$$

$$\alpha_{131} = (B_{12} + 2B_{66})\frac{r^2}{R^2} + (A_{12})\frac{1}{R}$$

$$\alpha_{132} = -B_{11}$$

$$\alpha_{211} = -B_{66}\frac{r}{R^2} - A_{12}\frac{r}{R} - B_{12}\frac{r}{R^2} - A_{66}\frac{r}{R}$$

$$\alpha_{221} = -A_{22}\frac{r^2}{R^2} - 2B_{22}\frac{r^2}{R^3} - D_{22}\frac{r^2}{R^4}$$

$$\alpha_{222} = A_{66} + 2D_{66}\frac{1}{R^3} - 3B_{66}\frac{1}{R}$$
$$\alpha_{231} = -D_{22}\frac{r^3}{R^4} - B_{22}\frac{r}{R} - B_{12}\frac{r\left(r^2+1\right)}{R^3} - A_{22}\frac{r}{R^2}$$
$$\alpha_{232} = (D_{12} + 2D_{66})\frac{r}{R^2} + (B_{12} + 2B_{66})\frac{r}{R}$$
$$\alpha_{311} = -B_{12}\frac{r^2}{R^2} + 2B_{66}\frac{r^2}{R^2} - A_{12}\frac{1}{R}$$
$$\alpha_{312} = B_{11}$$
$$\alpha_{321} = -D_{22}\frac{r^3}{R^4} - A_{22}\frac{r}{R^2} - B_{22}\left(\frac{r^3+r}{R^3}\right)$$
$$\alpha_{322} = (D_{12} + 4D_{66})\frac{r}{R^2} + (B_{12} + 2B_{66})\frac{r}{R}$$
$$\alpha_{331} = -D_{22}\frac{r^4}{R^4} - 2B_{22}\frac{r^2}{R^3} - A_{22}\frac{1}{R^2}$$
$$\alpha_{332} = 2D_{22}\frac{1}{R^2} + 4D_{66}\frac{r^2}{R^2} + 2B_{12}\frac{1}{R}$$
$$\alpha_{333} = -D_{11}$$

References

1. Soldatos, K.P., Hadjigeorgiou, V.P.: Three-dimensional solution of the free vibration problem of homogeneous isotropic cylindrical shells and panels. J. Sound Vib.Vib. **137**(3), 369–384 (1990). https://doi.org/10.1016/0022-460X(90)90805-A
2. Zukas, J.A., Vinson, J.R.: Laminated transversely isotropic cylindrical shells. J. Appl. Mech. **38**(2), 400–407 (1971). https://doi.org/10.1115/1.3408789
3. Spillers, W.R.: A laminated thin cylindrical shell under axisymmetric static loading. Int. J. Mech. Sci. **9**(12), 863–871 (1967). https://doi.org/10.1016/0020-7403(67)90012-4
4. Bert, C.W., Birman, V.: Parametric instability of thick, orthotropic, circular cylindrical shells. Acta Mech. Mech. **71**(61–76), 71 (1988). https://doi.org/10.1007/BF01173938
5. Khalili, S.M.R., Davar, A., Fard, K.M.: Free vibration analysis of homogeneous isotropic circular cylindrical shells based on a new three-dimensional refined higher-order theory. Int. J. Mech. Sci. **56**(1), 1–25 (2012). https://doi.org/10.1016/j.ijmecsci.2011.11.002
6. Li, H., Liu, D., Li, P., Zhao, J., Han, Q., Wang, Q.: A unified vibration modeling and dynamic analysis of FRP-FGPGP cylindrical shells under arbitrary boundary conditions. Appl. Math. Model. **97**, 69–80 (2021). https://doi.org/10.1016/j.apm.2021.03.054
7. Baghbadorani, A.A., Kiani, Y.: Free vibration analysis of functionally graded cylindrical shells reinforced with graphene platelets. Compos. Struct.Struct. **276**, 114546 (2021). https://doi.org/10.1016/j.compstruct.2021.114546
8. Qin, B., Wang, Q., Zhong, R., Zhao, X., Shuai, C.: A three-dimensional solution for free vibration of FGP-GPLRC cylindrical shells resting on elastic foundations: a comparative and parametric study. Int. J. Mech. Sci. **187**, 105896 (2020). https://doi.org/10.1016/j.ijmecsci.2020.105896
9. Azarafza, R., Davar, A., Fayez, M.S., Jam, J.E.: Free vibration of grid-stiffened composite cylindrical shell reinforced with carbon nanotubes. Mech. Compos. Mater. **56**, 505–522 (2020). https://doi.org/10.1007/s11029-020-09899-x
10. Zhang, Y., Jin, G., Chen, M., Ye, T., Liu, Z.: Isogeometric free vibration of sector cylindrical shells with carbon nanotubes reinforced and functionally graded materials. Results Phys. **16**, 102889 (2020). https://doi.org/10.1016/j.rinp.2019.102889
11. Tang, Q., Li, C., Wen, B.: Analysis on forced vibration of thin-wall cylindrical shell with nonlinear boundary condition. Shock. Vib.Vib. **1**, 8978932 (2016). https://doi.org/10.1155/2016/8978932
12. Sofiyev, A.H., Kuruoglu, N.: Buckling and vibration of shear deformable functionally graded orthotropic cylindrical shells under external pressures. Thin-Walled Struct. **78**, 121–130 (2014). https://doi.org/10.1016/j.tws.2014.01.009
13. Alibeigloo, A., Jafarian, H.: Three-dimensional static and free vibration analysis of carbon nano tube reinforced composite cylindrical shell using differential quadrature method. Int. J. Appl. Mech. **8**(03), 1650033 (2016). https://doi.org/10.1142/S1758825116500332
14. Miao, X., Li, C., Jiang, Y.: Free vibration analysis of metal-ceramic matrix composite laminated cylindrical shell reinforced by CNTs. Compos. Struct.Struct. **260**, 113262 (2021). https://doi.org/10.1016/j.compstruct.2020.113262
15. Babaei, M.J., Jafari, A.A.: Effect of thermal environment on the free vibration of functionally graded carbon nanotubes cylindrical-conical shell. J. Therm. Stress. **47**(1), 35–58 (2024). https://doi.org/10.1080/01495739.2023.2271525
16. Baltacıoğlu, A.K., Civalek, Ö.: Vibration analysis of circular cylindrical panels with CNT reinforced and FGM composites. Compos. Struct.Struct. **202**, 374–388 (2018). https://doi.org/10.1016/j.compstruct.2018.02.024
17. Chakraborty, S., Dey, T., Kumar, R.: Stability and vibration analysis of CNT-reinforced functionally graded laminated composite cylindrical shell panels using semi-analytical approach. Compos. Part B Eng. **168**, 1–14 (2019). https://doi.org/10.1016/j.compositesb.2018.12.051

18. Hosseini, H., Kolahchi, R.: Seismic response of functionally graded-carbon nanotubes-reinforced submerged viscoelastic cylindrical shell in hygrothermal environment. Phys. E Low-dimens. Syst. Nanostruct. **102**, 101–109 (2018). https://doi.org/10.1016/j.physe.2018.04.037
19. Alibeigloo, A., Zanoosi, A.P.: Thermo-electro-elasticity solution of functionally graded carbon nanotube reinforced composite cylindrical shell embedded in piezoelectric layers. Compos. Struct.Struct. **173**, 268–280 (2017). https://doi.org/10.1016/j.compstruct.2017.04.027
20. Kiani, F., Hekmatifar, M., Toghraie, D.: Analysis of forced and free vibrations of composite porous core sandwich cylindrical shells and FG-CNTs reinforced face sheets resting on visco-Pasternak foundation under uniform thermal field. J. Braz. Soc. Mech. Sci. Eng. **42**(10), 504 (2020). https://doi.org/10.1007/s40430-020-02591-0
21. Pradhan, S.C., Loy, C.T., Lam, K.Y., Reddy, J.N.: Vibration characteristics of functionally graded cylindrical shells under various boundary conditions. Appl. Acoust. **61**(1), 111–129 (2000). https://doi.org/10.1016/S0003-682X(99)00063-8
22. Wang, Y., Wu, D.: Free vibration of functionally graded porous cylindrical shell using a sinusoidal shear deformation theory. Aerosp. Sci. Technol.. Sci. Technol. **66**, 83–91 (2017). https://doi.org/10.1016/j.ast.2017.03.003
23. Chen, J., Ahmed, M.: On the large deformation vibrations of Graphene platelets-reinforced composite plates located on elastic foundation: nonlinear analytical method. Acta Mech. Mech. (2024). https://doi.org/10.1007/s00707-024-03969-0
24. KhoddamiMaraghi, Z., Arshid, E.: On the vibrational behavior of variable thickness FG porous beams with graphene-reinforced nanocomposite facesheets. Acta Mech. Mech. (2024). https://doi.org/10.1007/s00707-024-03987-y
25. Yan, G., Babaei, H.: Nonlinear vibration and buckling analyses of sandwich arch with titanium alloy face sheets and a porosity-dependent GPLRC core. Acta Mech. **235**(8), 5431–5449 (2024). https://doi.org/10.1007/s00707-024-03982-3
26. Cho, J.R.: Investigation of nonlinear free vibration of FG-CNTRC cylindrical panels resting on elastic foundation. Struct. Eng. Mech. Int. J. **88**(5), 439–449 (2023). https://doi.org/10.12989/sem.2023.88.5.439
27. Allahyari, S.M.R., Shokravi, M., Murmy, T.T.: Modeling of truncated nanocompositeconical shell structures for dynamic stability response. Struct. Eng. Mech.. Eng. Mech. **91**(3), 325–334 (2024). https://doi.org/10.12989/sem.2024.91.3.325
28. Cui, Z., Yuan, Z., Xi, C.: Engineering the future: exploring the dynamic behavior of nanocomposite porous beams under the influence of nanoparticles. Struct. Eng. Mech.. Eng. Mech. **92**(5), 513–520 (2024). https://doi.org/10.12989/sem.2024.92.5.513
29. Özdemir, Ö., Esen, İ, Ural, H.: Vibration response of rotating carbon nanotube reinforced composites in thermal environment. Steel Compos. Struct.Struct. **47**(1), 1–17 (2023). https://doi.org/10.12989/scs.2023.47.1.001
30. Zhang, Y., Zhao, Q., Han, Q., Bohlooli, N.: Free vibration analysis of a laminated trapezoidal plate with GrF-PMC core and wavy CNT-reinforced face sheets. Steel Compos. Struct.Struct. **48**(3), 275–291 (2023). https://doi.org/10.12989/scs.2023.48.3.275
31. Long, C., Wang, D., Xiang, H.B.: Static and dynamic bending of ball reinforced by CNTs considering agglomeration effect. Steel Compos. Struct.Struct. **48**(4), 419–428 (2023). https://doi.org/10.12989/scs.2023.48.3.419
32. Wu, X.: Nonlinear finite element vibration analysis of functionally graded nanocomposite spherical shells reinforced with graphene platelets. Adv. Nano Res. **15**(2), 141–153 (2023). https://doi.org/10.12989/anr.2023.15.2.141
33. Wang, X., Guo, X., Babaei, M., Fili, R., Farahani, H.: Natural frequency analysis of joined conical-cylindrical-conical shells made of graphene platelet reinforced composite resting on Winkler elastic foundation. Adv. Nano Res. **15**(4), 367–384 (2023). https://doi.org/10.12989/anr.2023.15.4.367
34. Alambeigi, K., Mohammadimehr, M., Bamdad, M.: An analytical study on free vibration of magneto electro micro sandwich beam with FG porous core on Vlasov foundation. Adv. Nano Res. **15**(5), 423 (2023). https://doi.org/10.12989/anr.2023.15.5.423
35. Ding, H.X., Liu, H.B., She, G.L., Wu, F.: Wave propagation of FG-CNTRC plates in thermal environment using the high-order shear deformation plate theory. Comput. Concr.. Concr. **32**(2), 207–215 (2023). https://doi.org/10.12989/cac.2023.32.2.207
36. Emdadi, M., Mohammadimehr, M., Navi, B.R.: The surface stress effects on the buckling analysis of porous microcomposite annular sandwich plate based on HSDT using Ritz method. Comput. Concr.. Concr. **32**(5), 439 (2023). https://doi.org/10.12989/cac.2023.32.5.439
37. Wu, H., Kitipornchai, S., Yang, J.: Free vibration and buckling analysis of sandwich beams with functionally graded carbon nanotube-reinforced composite face sheets. Int. J. Struct. Stab. Dyn.Struct. Stab. Dyn. **15**(07), 1540011 (2015). https://doi.org/10.1142/S0219455415400118
38. Shu, C., Du, H.: Free vibration analysis of laminated composite cylindrical shells by DQM. Compos. Part B Eng. **28**(3), 267–274 (1997). https://doi.org/10.1016/S1359-8368(96)00052-2

Publisher's Note Springer Nature remains neutral with regard to jurisdictional claims in published maps and institutional affiliations.

Springer Nature or its licensor (e.g. a society or other partner) holds exclusive rights to this article under a publishing agreement with the author(s) or other rightsholder(s); author self-archiving of the accepted manuscript version of this article is solely governed by the terms of such publishing agreement and applicable law.